Temperature effects on fatigue delamination behavior in thermoset composite laminates

Yao, Liaojun; Chuai, Mingyue; Li, Hanyue; Chen, Xiangming; Quan, Dong; Alderliesten, R. C.; Beyens, M.

DOI
10.1016/j.engfracmech.2023.109799

Publication date
2024

Document Version
Final published version

Published in
Engineering Fracture Mechanics

Engineering Fracture Mechanics 295 (2024) 109799

Contents lists available at ScienceDirect

Engineering Fracture Mechanics

journal homepage: www.elsevier.com/locate/engfracmech

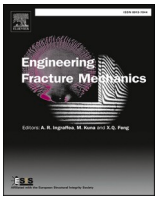

Temperature effects on fatigue delamination behavior in thermoset composite laminates

Liaojun Yao [a,b,*], Mingyue Chuai [a], Hanyue Li [a], Xiangming Chen [b], Dong Quan [c,d], R.C. Alderliesten [d], M. Beyens [d]

[a] Department of Astronautics Science and Mechanics, Harbin Institute of Technology, Harbin, PR China
[b] National Key Laboratory of Strength and Structural Integrity, Aircraft Strength Research Institute of China, Xi'an, PR China
[c] Key Laboratory for Liquid-Solid Structural Evolution and Processing of Materials, Shandong University, PR China
[d] Structural Integrity and Composite Group, Faculty of Aerospace Engineering, Delft University of Technology, the Netherlands

ARTICLE INFO

Keywords:
Fatigue delamination growth
Fiber bridging retardation
Temperature effects
Polymer-matrix composites

ABSTRACT

Temperature can significantly affect fatigue delamination growth (FDG) behavior in composites, while fiber bridging has been frequently reported during FDG. The focus of this study was therefore on investigating temperature effects on FDG behavior with fiber bridging. Mode I fatigue delamination experiments were conducted on a thermoset composite laminates M30SC/DT120 at different temperatures. The Paris relation and fatigue resistance curve (i.e. fatigue *R*-curve) were used to interpret bridging effects on FDG behavior and to explore temperature effects on fiber bridging development. A modified Paris relation was employed to determine the effects of temperature on the intrinsic FDG behavior at the crack front excluding fiber bridging. The Paris interpretations clearly demonstrate that fiber bridging can significantly retard FDG behavior at different temperatures. Temperature can have different effects on fiber bridging development and the intrinsic FDG behavior. Particularly, elevated temperature can promote more bridging fibers, whereas decreased temperature has negligible influence on fiber bridging. When looking at the intrinsic delamination resistance, mode I FDG can accelerate at elevated temperature but decrease at freezing temperature. Fractographic examinations indicate that fiber/matrix interface debonding is the dominant damage mechanism in mode I FDG at different temperatures. Elevated temperature can lead to the weakening of interface adhesion, contributing to faster intrinsic mode I FDG behavior and more fiber bridging development. And a semi-empirical fatigue model based on normalization was finally proposed to determine mode I intrinsic FDG behavior at different temperatures for engineering applications.

1. Introduction

Carbon fiber reinforced polymer composites have been widely used in aerospace industry for their excellent mechanical properties, designability, and weight-saving potential. However, these materials are vulnerable to delamination growth, due to lack of through-thickness reinforcement. The initiation and propagation of this damage can gradually cause strength/stiffness degradation, and may finally result in catastrophic failure of a composite structure during its long-term service life. In addition, the US Federal Aviation

* Corresponding author at: Department of Astronautics Science and Mechanics, Harbin Institute of Technology, Harbin, PR China.
E-mail address: L.Yao@hit.edu.cn (L. Yao).

https://doi.org/10.1016/j.engfracmech.2023.109799
Received 17 September 2023; Received in revised form 20 November 2023; Accepted 8 December 2023
Available online 14 December 2023
0013-7944/

Administration (FAA) has introduced *a slow crack growth principle* for the certification of composite and adhesively bonded structures originally in 2009 [1]. As a result, increasing attention has been given into how to appropriately represent delamination behavior of composites under fatigue loading [2–5]. Both the European Structural Integrity Society Technical Committee 4 (ESIS TC4) and the American Society for Testing and Materials, International, Subcommittee D30.06 (ASTM D30.06) have performed separate round-robin test programs for the purpose of developing a test standard for mode I FDG in composites [2–5]. And a series of factors, including control modes (i.e. load control vs. displacement control), test frequency, and fatigue crack growth rate *da/dN* calculation approaches (i.e. two-point and seven-point fit), have been thoroughly investigated and discussed in these studies. Despite several attempts to come to a test standard through these round-robin exercises, no protocol yet has been developed successfully. One dominant reason for the absence of consensus on the test standard attributes to the occurrence of fiber bridging in mostly unidirectional composites, shielding the crack front and resulting in apparently higher delamination resistance. As a result, how to appropriately represent fiber-bridged FDG behavior is a key issue for the development of this test standard [6].

The presence of fiber bridging in delamination growth of carbon fiber reinforced polymer composites mainly attributes to fiber nesting between adjacent layers, which could be promoted by weak fiber/matrix interfaces [7]. In quasi-static delamination, the contribution of fiber bridging was generally illustrated through *R*-curves, plotting delamination resistance against crack propagation length $G_C(a\text{-}a_0)$, and bridging laws, comprising bridging closure stress against crack opening displacement $\sigma_{br}(\delta)$ [8–13]. According to the previous studies [4,8,9], this shielding mechanism not only occurs in quasi-static delamination, but also exists in FDG of composites.

Paris relation Eq.(1) and its variants, correlating *da/dN* with the strain energy release rate (*SERR*) *G*, have been generally used in FDG studies [2–5,14]. It has been reported several times that fiber bridging has significant retardation effects on FDG behavior [8,15,16]. This makes it impossible to use a single Paris resistance curve to appropriately represent FDG behavior, indifferent of whether one uses the *SERR* range $\Delta\sqrt{G}$ or the maximum *SERR* G_{max} in fatigue data interpretations. According to the J-integral concept [11,12,17], the presence of bridging fibers can store a large amount of strain energy during delamination, thus alleviating stress concentration around delamination front. To account for bridging retardation, scholars [18] have attempted to make correlations between the curve-fitting parameters and crack growth length to have an empirical Paris-type correlation to characterize fiber-bridged FDG behavior.

$$\frac{da}{dN} = C(\Delta G)^n = C\left[\left(\sqrt{G_{max}} - \sqrt{G_{min}}\right)^2\right]^n \tag{1}$$

where *C*, *n* are curve-fitting parameters; G_{max} and G_{min} respectively represent the maximum and minimum *SERRs* of a fatigue loading cycle.

Several researchers tended to treat bridging retardation effects on FDG behavior as data scatter [4,19], thus adopting normalization methods to limit this scatter. Murri et al [4] used a normalized Paris relation, in which G_{max} was normalized with the quasi-static delamination resistance. This study demonstrated that the use of this normalized *SERR* can reduce data scatter in FDG studies. A similar concept was also employed by other researchers in fiber-bridged FDG characterization [16,20–22]. However, it has been evidenced that [8] the amounts of bridging fibers generated in fatigue differ from quasi-static. Hence, one should consider the fatigue *R*-curve, rather than the quasi-static, in FDG normalization [8,20,21,23].

Instead of using *R*-curve normalization, both Gregory et al [24] and Farmand-Ashtiani et al [25] reported good correlations between FDG rate *da/dN* and the *SERR* at the crack front. Furthermore, it has been evidenced that [23] damage mechanisms at the crack front remain the same with delamination propagation, regardless of fiber bridging development. As a result, it can be deduced that FDG behavior at the crack front remains self-similar with fiber bridging development, making the *SERR* at the crack front an appropriate similitude parameter to represent this similarity in fiber-bridged FDG characterization. Accordingly, a modified Paris relation has been successfully proposed by the authors to explore FDG behavior with large-scale fiber bridging [26]:

$$\frac{da}{dN} = C\left(\Delta G_{eff}\right)^n = C\left[\frac{G_0}{G_{IC}(a-a_0)}\Delta G\right]^n \tag{2}$$

where $G_{IC}(a\text{-}a_0)$ represents fatigue resistance increase because of fiber bridging; G_0 is fatigue resistance at the crack front excluding fiber bridging, which could be determined via fatigue *R*-curve $G_{IC}(a\text{-}a_0)$ extrapolation.

Since this modified Paris relation Eq.(2) can provide a single master resistance curve in determining FDG behavior, it agrees well with the similitude hypothesis [23,26]. Furthermore, because using Eq.(2) indeed describes fatigue delamination characteristic at the crack front, it can be therefore considered as the intrinsic delamination resistance excluding fiber bridging. This intrinsic resistance curve indeed represents the upper bound of all curves, which in engineering serves as the worst case for composite structural designs.

However, before rushing into conclusions, such a proposal must be evaluated further for two reasons: scientifically, the interplay between crack front characteristics and fiber bridging must be thoroughly studied in different conditions, while for engineering purposes, the influence of environmental factors should be appropriately understood, as they are known to have significant influence on FDG behavior [14,27,28]. The most important environmental factor on interlaminar resistance is evidently temperature [14]. And a temperature range of −50℃ to 80℃ has been frequently employed in the previous studies [24,27,28], which is assumed to well cover the operating temperatures for composite structures in the aeronautical applications.

Charalambous et al [27] experimentally investigated temperature effects on the mixed-mode delamination growth behavior under both quasi-static and cyclic loading, observing an increase in static delamination resistance at elevated temperature (i.e. 80℃), attributed to increased matrix ductility. On the contrary, FDG can accelerate with increased temperature, due to a weaker fiber/matrix

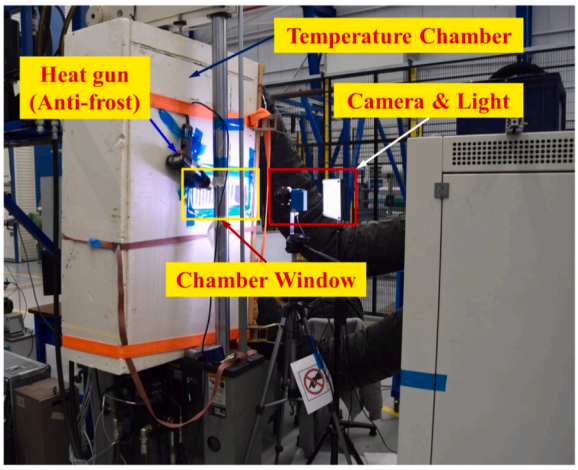

(a)

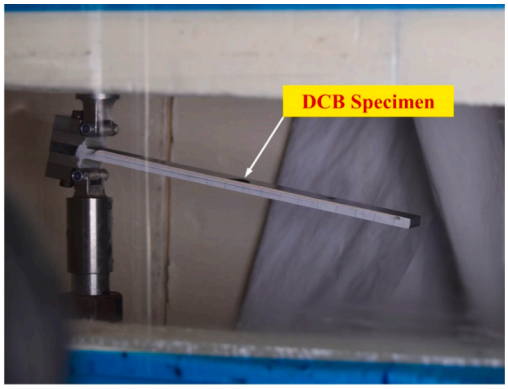

(b)

Fig. 1. Experimental setup for FDG test at different temperatures. (a) Overall experimental setup; (b) A detail view of DCB specimen in the temperature chamber.

interface bond at elevated temperature. Coronado et al [28] experimentally examined mode I quasi-static and fatigue delamination resistance at freezing temperatures, observing both to reduce, explained by more brittle fracture surface features via fractographic examinations. In contrast, Gregory et al [29] reported that no clear trend was found in quasi-static delamination resistance with respect to temperature, while a significant negative dependence was observed in FDG. In another study [24], they adopted a bridging law to extract the *SERR* at the crack front to study FDG dependence on temperature. It was reported that FDG can increase with elevated temperature. Similarly, as also illustrated by Sjogren et al [30], elevated temperature can not only increase the FDG rate, but also promote more fiber bridging affecting the FDG behavior.

While currently, subject of another round robin within ESIS TC4, the hypothesis in the current study is that temperature has important effects on delamination resistance, and through the fiber/matrix interface adhesion also a clear influence on the formation of fiber bridging. As a result, answers are needed on the following key questions:

1. What effect does the temperature have on the development of fiber bridging during mode I FDG in composites, associated to fiber/matrix interface adhesion?

2. What effect does the temperature have on the intrinsic FDG resistance when fiber bridging is excluded, associated to fiber/matrix interface adhesion at the crack front?

3. How should FDG behavior at different temperatures be well represented for the perspective of engineering designs?

To answer these questions, mode I fatigue delamination experiments were conducted at different temperatures, ranging from −40℃ to 80℃, at the stress ratio $R = 0.5$. Both the Paris relation Eq.(1) and the modified Paris relation Eq.(2) were respectively used to interpret these FDG data. Particularly, the Paris interpretations, incorporated with the fatigue *R*-curves, were used to explore bridging effects on FDG behavior and temperature dependence of fiber bridging development. The modified Paris relation was applied to determine temperature effects on the intrinsic FDG behavior excluding fiber bridging. Fractographic examinations were subsequently conducted to determine the damage mechanisms in FDG at different temperatures, to assist the interpretations of temperature dependence on the intrinsic FDG behavior and fiber bridging development. Finally, a semi-empirical relation accounting for data

Table 1
Test matrix for FDG at different temperatures.

T	Specimen	*R*	Fatigue pre-crack length [mm]
−40℃	−40℃ Spe	0.5	4.0;13.6;21.3;28.6;36.6;46.2;55.0;65.4;76.3;90.4;102.5
RT	RT Spe-1		3.4;13.5;21.5;39.0;51.5;63.0;76.6;91.0
	RT Spe-2		3.7;15.6;25.8;35.1;46.1;57.1;70.0;84.4;100.7
50℃	50℃ Spe		3.7;15.1;25.2;36.6;48.7;57.2;72.4;89.1
80℃	80℃ Spe-1		3.5;14.4;25.9;39.1;53.2;68.9;87.0;104.3
	80℃ Spe-2		3.3;15.3;28.8;41.3;57.9;74.9;91.8;101.8

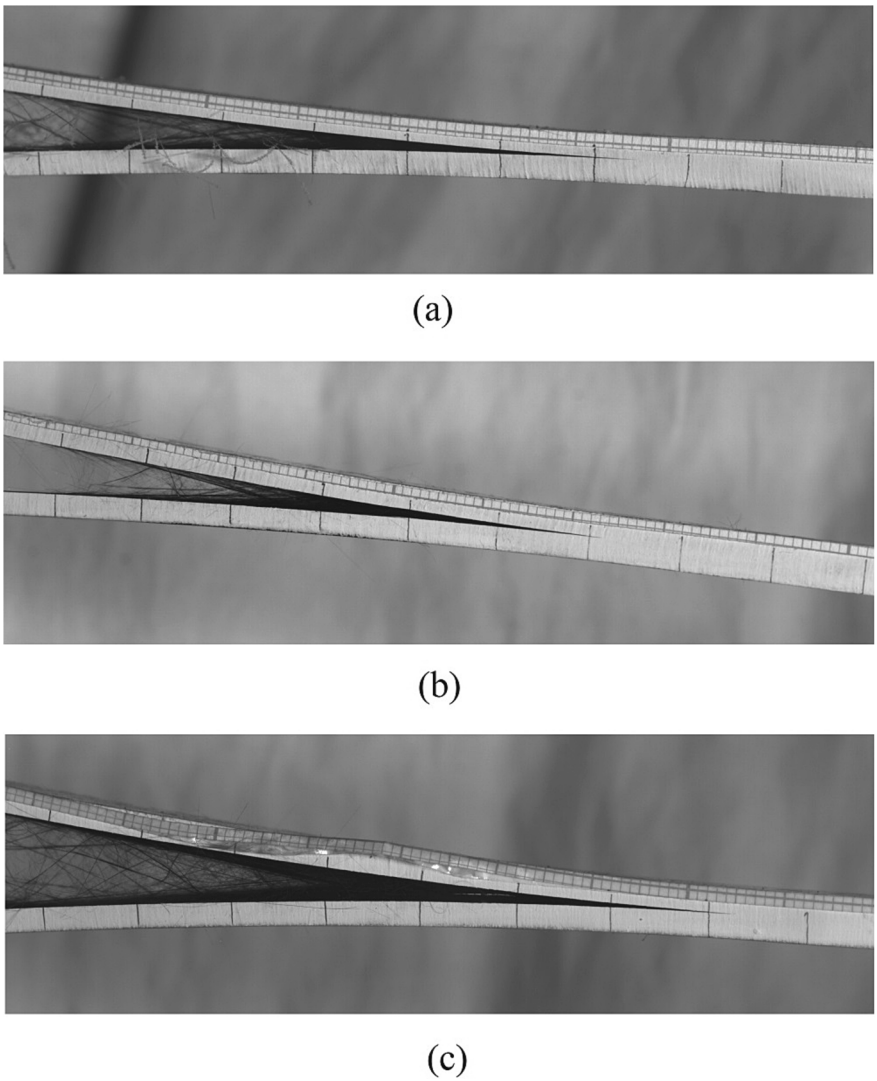

Fig. 2. Fiber bridging in mode I FDG of composites at different temperatures. (a) −40℃; (b) RT; (c) 80℃.

scatter was developed to represent mode I FDG behavior at different temperatures for engineering designs.

2. Specimens, experimental setup and data reduction

The material used here was carbon/epoxy prepreg M30SC/DT120 (high strength and modulus carbon fiber/toughened thermo-setting epoxy). Mechanical properties of the cured material are referred to literature [31]. Composite laminates were laid in the designed stacking sequence, i.e. $[0_{16}//0_{16}]$. A Teflon insert with 12.7 μm thickness was placed in the middle plane to introduce an initial delamination, typically around $a_0 = 60$ mm. Laminates were cured in the autoclave at a pressure of 6 bars and curing

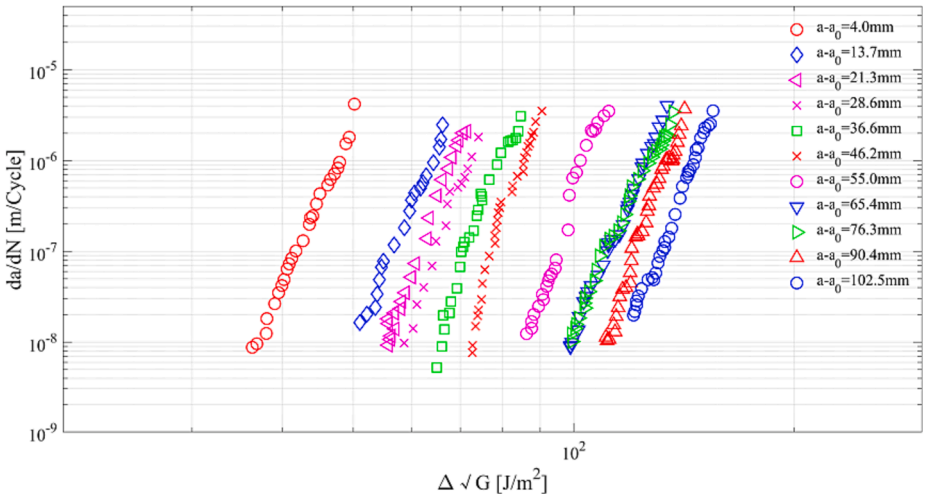

Fig. 3. Fiber-bridged FDG at −40℃ interpreted via the Paris relation.

temperature of 120℃ for 90 min. After curing, the laminates were C-scanned for imperfections. Samples were taken from these areas where no imperfections were identified.

Unidirectional double cantilever beam (DCB) specimens, $L = 200$ mm length by $B = 25$ mm width with thickness of $h = 5$ mm, were cut from the laminates panel with a diamond-coated cutting machine. One edge of each DCB specimen was coated with a thin layer of typewriter correction fluid to enhance the visibility of delamination front during the tests. A strip of grid paper was pasted on the coated side of the sample to aid in measuring crack propagation length during the tests.

All mode I fatigue delamination experiments were conducted on a 15kN MTS servo-hydraulic test machine under displacement control at a frequency of 5 Hz with a stress ratio of $R = 0.5$. The load, displacement and number of cycles were automatically stored in an Excel file enabling data reduction after the test. A temperature chamber, built in the laboratory with temperature capacity range from −40℃ to 80℃, was used to generate the required temperatures (i.e. −40℃, RT, 50℃ and 80℃) during the entire fatigue tests. Particularly, this chamber contains a window, in front of which a computer controlled digital camera system with high resolution was placed to monitor delamination propagation via automatically recording an image of the tested specimen at certain fatigue intervals. These recorded images could be analyzed to determine the fatigue delamination propagation length a-a_0 after the experiments. Inside of the chamber, a thermocouple was installed just above the specimen to measure the temperature to ensure there is a stable temperature throughout the entire fatigue test. To keep the monitor window from freezing during sub-zero fatigue delamination tests, a heat gun was added to act as anti-frost. Detail information of the experimental setup as well as the DCB specimen in the temperature chamber is demonstrated in Fig. 1.

To determine fatigue delamination behavior with different amounts of fiber bridging, as well as to have the fatigue R-curve exploring temperature effects on fiber bridging development, DCB specimens were repeatedly tested for several times with increased displacements keeping the stress ratio constant at $R = 0.5$. This specific test procedure has been introduced and used several times in the previous studies [8,18,23]. Typically, DCB specimen was first quasi-statically loaded to generate a really short natural crack front (around 2–3 mm), as well as to determine the minimum and maximum displacements used in the subsequent fatigue delamination test. One should note that FDG rate da/dN gradually decreases with decreasing $SERR$ in a displacement controlled fatigue test. Each test was therefore manually terminated in case of crack retardation. Subsequently, a monotonic loading–unloading cycle was performed on the tested specimen until the load–displacement curve becomes slightly nonlinear (i.e. avoiding new fiber bridging generation in quasi-static delamination) to evaluate the minimum and maximum displacements applied in the subsequent fatigue test sequence. This sequence was repeated multiple times until the maximum displacement capacity of the test machine was reached. With this test procedure, multiple delamination resistance curves were obtained, with each one representing delamination resistance equivalent to a specific fatigue pre-crack length, i.e. delamination length at which that particular fatigue test was initiated. Furthermore, fatigue fracture toughness at several fatigue delamination lengths can be determined with the information recorded at the nonlinear point according to this test procedure as well (i.e. forming the fatigue R-curve).

The Modified Compliance Calibration (MCC) method Eq.(3), recommended in the ASTM D5528-01 standard, was employed to calculate the $SERR$ G with the load, displacement and crack length information recorded in fatigue delamination tests. The 7-point Incremental Polynomial Method, recommended in the ASTM E647-00 standard, was used to fatigue crack growth rate da/dN calculation.

$$G = \frac{3P^2C^{(2/3)}}{2A_1Bh} \tag{3}$$

where P is the load; C is the compliance of the DCB specimen; A_1 is the slope of the curve in the graph where a/h is plotted against $C^{1/3}$.

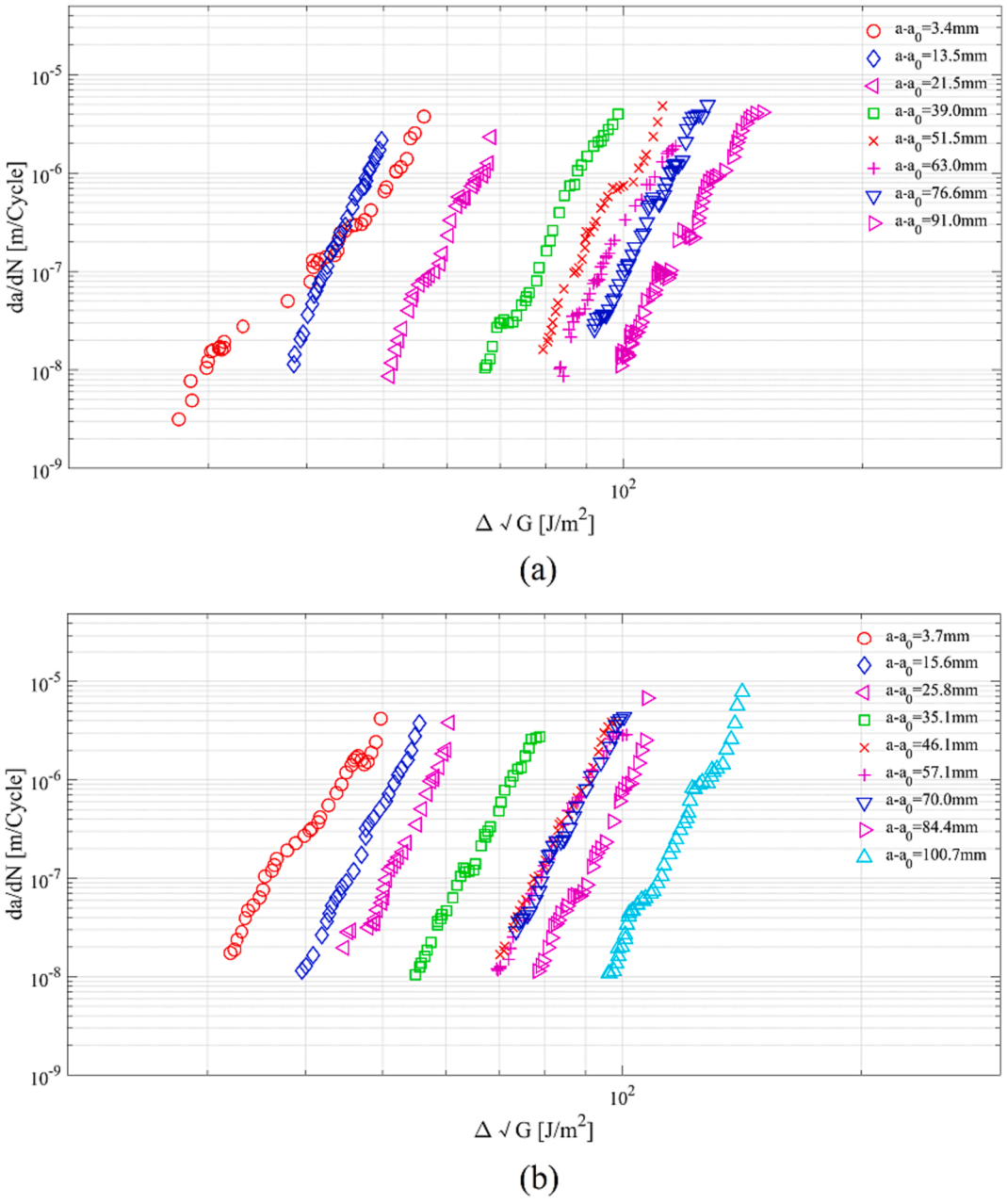

Fig. 4. Fiber-bridged FDG at RT interpreted via the Paris relation. (a) RT Spe-1; (b) RT Spe-2.

3. Results and discussions

A total number of 52 fatigue delamination tests have been conducted to explore temperature effects on mode I FDG behavior with fiber bridging. The test matrix is summarized in Table 1. There are two DCB specimens were repeatedly tested at RT and 80℃. And these specimens were entitled as Spe-1 and Spe-2 for each temperature. The experimental fatigue data of −40℃, RT and 80℃ were interpreted to explore temperature effects on FDG behavior. And the results of 50℃ were used to verify the validity of using the proposed semi-empirical correlation in determining FDG behavior at different temperatures.

3.1. Temperature dependence of FDG behavior including fiber bridging

Significant amounts of bridging fibers were observed during mode I FDG at all temperatures, as illustrated in Fig. 2. And these bridging fibers are present in terms of a single one or a cluster of fibers in the wake of the delamination front.

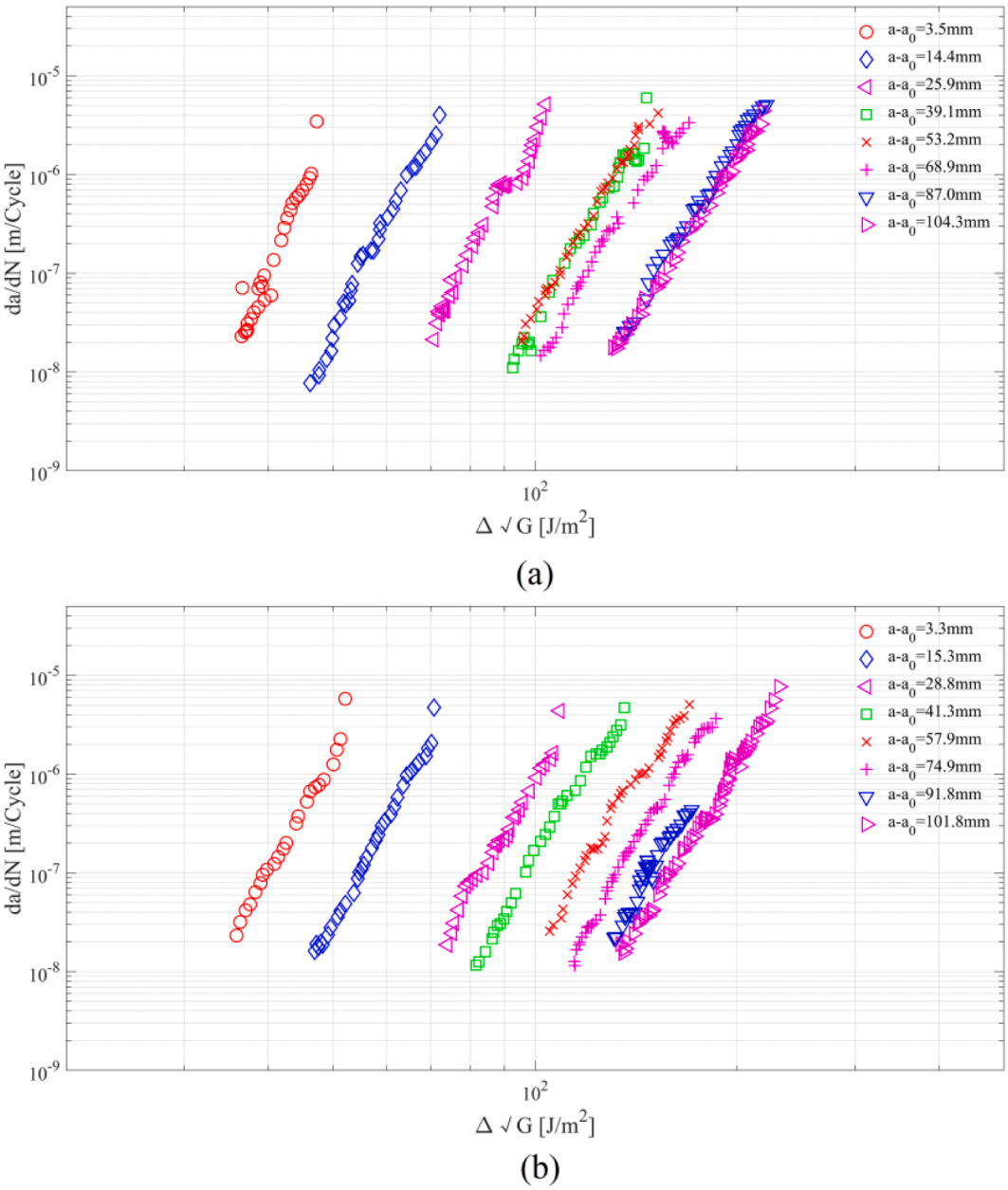

Fig. 5. Fiber-bridged FDG at 80℃ interpreted via the Paris relation. (a) 80℃ Spe-1; (b) 80℃ Spe-2.

Figs. 3–5 summarize all fatigue data at different temperatures interpreted via the Paris relation Eq.(1). These results clearly demonstrate that fiber bridging has significant retardation effects on mode I FDG behavior. Particularly, the Paris resistance curves can gradually shift from left to right in these graphs, and finally tend to converge into a narrow band region with fatigue crack propagation. As discussed in literature [8,18], fiber bridging is the main reason for this downwards shift. A large portion of *SERR* put into the system could be cyclically applied and released on these bridging fibers rather than on the crack front, i.e. shielding the delamination front. However, fiber bridging can saturate once crack propagation exceeds a certain level. This means the generation of new bridging fibers at the advancing crack front can balance the final failure of bridging fibers at the end of the bridging zone. Consequently, the *SERR* applied in these bridging fibers can keep constant more or less in FDG with really long fatigue pre-cracks, finally making the resistance curves collapse into a narrow band region.

According to the results illustrated in Figs. 3–5, one can make conclusions as:

(1) Fiber bridging, acting as an important shielding mechanism, can not only be present in mode I FDG at RT, but also exist at freezing and elevated temperatures;

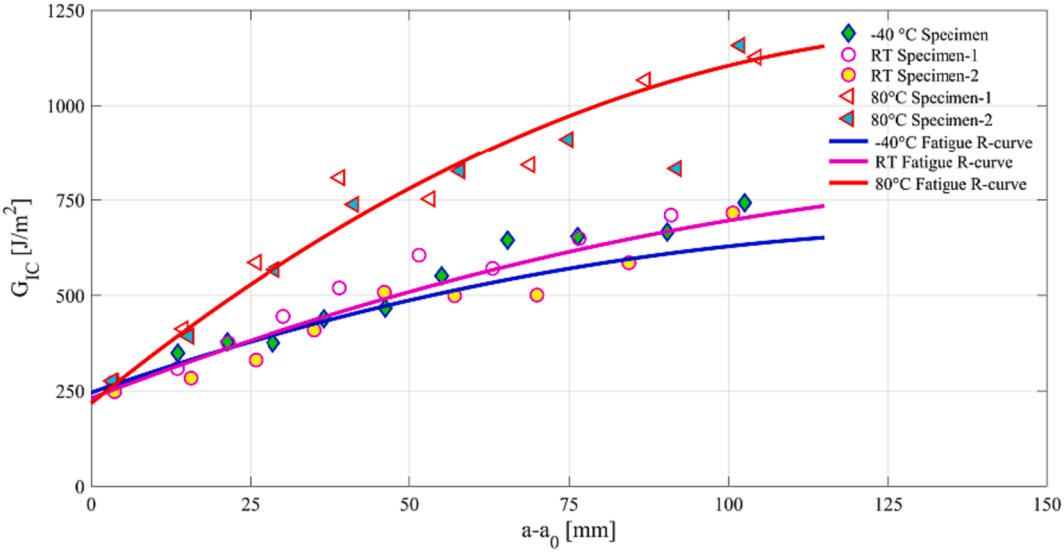

Fig. 6. Fatigue *R*-curves for mode I FDG at different temperatures.

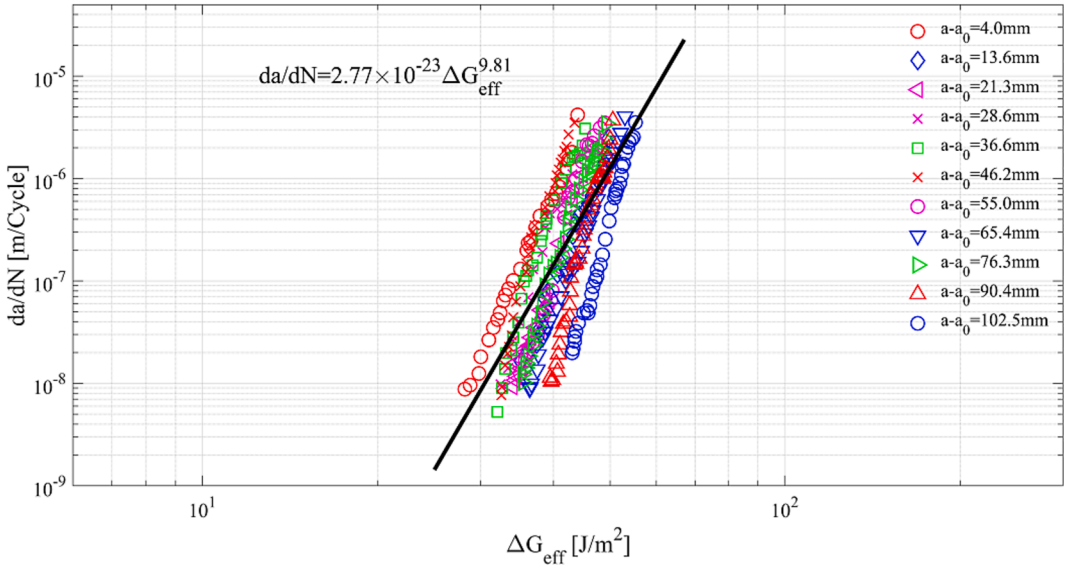

Fig. 7. Fatigue data of −40℃ interpreted via the modified Paris relation.

(2) The presence of fiber bridging can cause significant FDG retardation in different temperatures.

Referring to the *R*-curve concept frequently used in characterizing quasi-static delamination resistance with fiber bridging, fatigue *R*-curves were determined with the specific test procedure introduced in Section 2, to explore temperature effects on fiber bridging development. Fig. 6 illustrates these fatigue *R*-curves at different temperatures. It is clear that fatigue *R*-curve of each temperature can increase significantly with crack propagation, which can be well determined via a second-order polynomial fitting. Furthermore, these results also demonstrate that temperature has important influence on the shapes of fatigue *R*-curves, especially for the elevated 80℃. Particularly, the initiation fatigue delamination resistance at $a\text{-}a_0 = 0$ mm can decrease with temperature increase, i.e. 245.30 J/m^2 for −40℃, 230.78 J/m^2 for RT and 217.32 J/m^2 for 80℃. On the contrary, the magnitude of fatigue *R*-curve for 80℃ is much higher than that of the other temperatures, indicating more bridging fibers in FDG at 80℃ (more evidence to support this statement can been found in the SEM fractographic examinations on fatigue delamination surfaces in Section 3.3). The fatigue *R*-curves for −40℃ and RT generally looks the same or similar, indicating similar amounts of bridging fibers at these temperatures.

According to these fatigue *R*-curves illustrated in Fig. 6, it can be concluded that temperature has different influence on the initiation delamination resistance and the formation of fiber bridging during mode I FDG. The initiation delamination resistance can decrease with temperature increase. More bridging fibers can be present at elevated temperature, whereas decreased temperature has

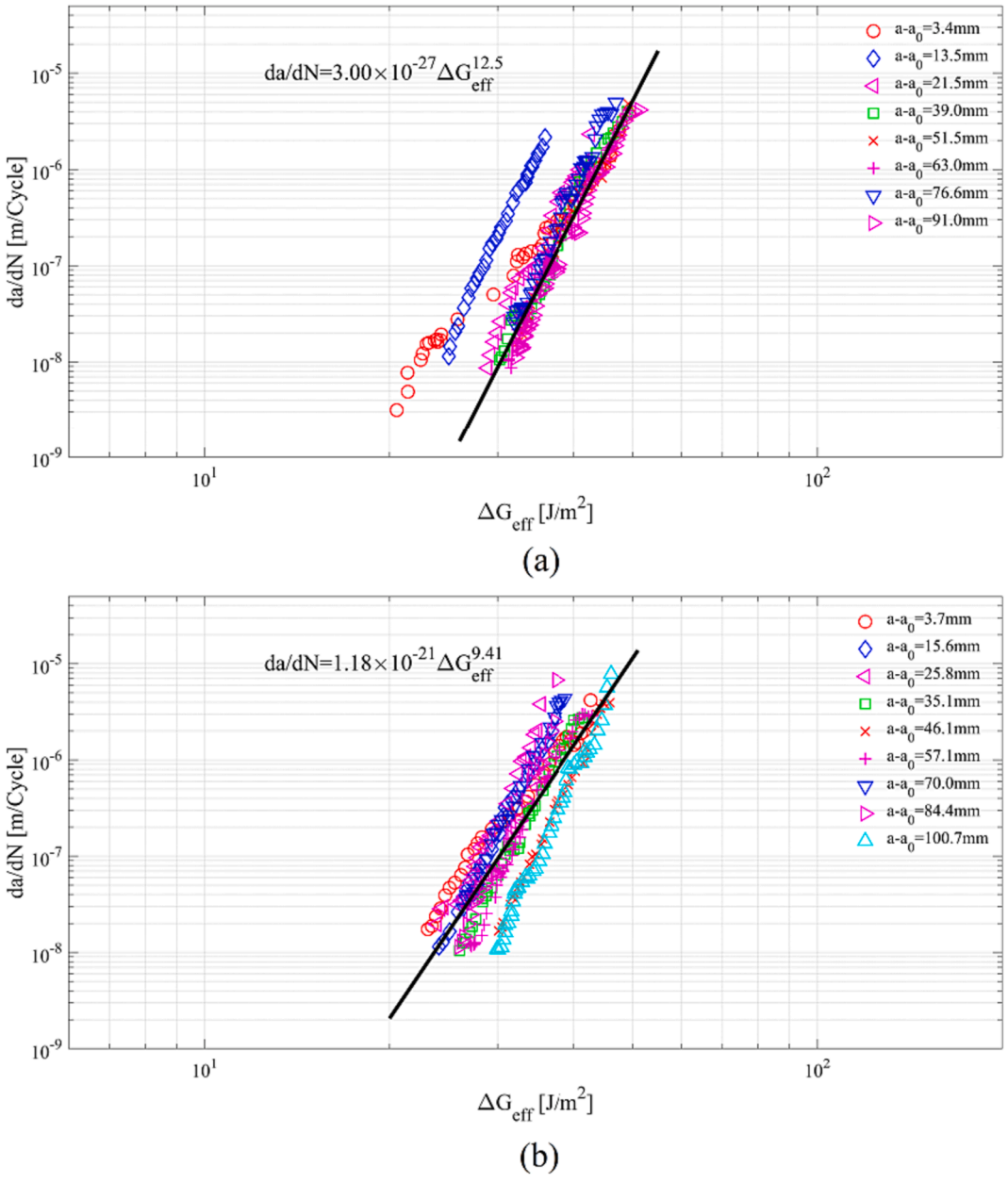

Fig. 8. Fatigue data of RT interpreted via the modified Paris relation. (a) RT Spe-1; (b) RT Spe-2.

negligible influence on fiber bridging generation. The physical reasons for this difference in temperature dependence of initiation delamination resistance and fiber bridging development will be carefully discussed as follows via SEM examinations on fatigue delamination fracture surfaces.

3.2. Temperature effects on the intrinsic FDG behavior excluding fiber bridging

According to the above Paris interpretations, bridging retardation effects on mode I FDG behavior at different temperatures have been discussed. People then may ask a question that *what are temperature effects on the intrinsic delamination resistance at the crack front*. However, one cannot make a clear conclusion on this point via the above Paris interpretations.

All experimental fatigue data were therefore re-analyzed via the modified Paris relation, as illustrated in Figs. 7–9. It is clear that fatigue delamination with different amounts of bridging fibers can converge into a narrow band region at each temperature using Eq. (2) in data reduction, contributing to a master resistance curve in representing mode I FDG behavior, which agrees well with the similitude hypothesis [32–34]. Furthermore, these interpretations make it possible to explore temperature effects on the intrinsic

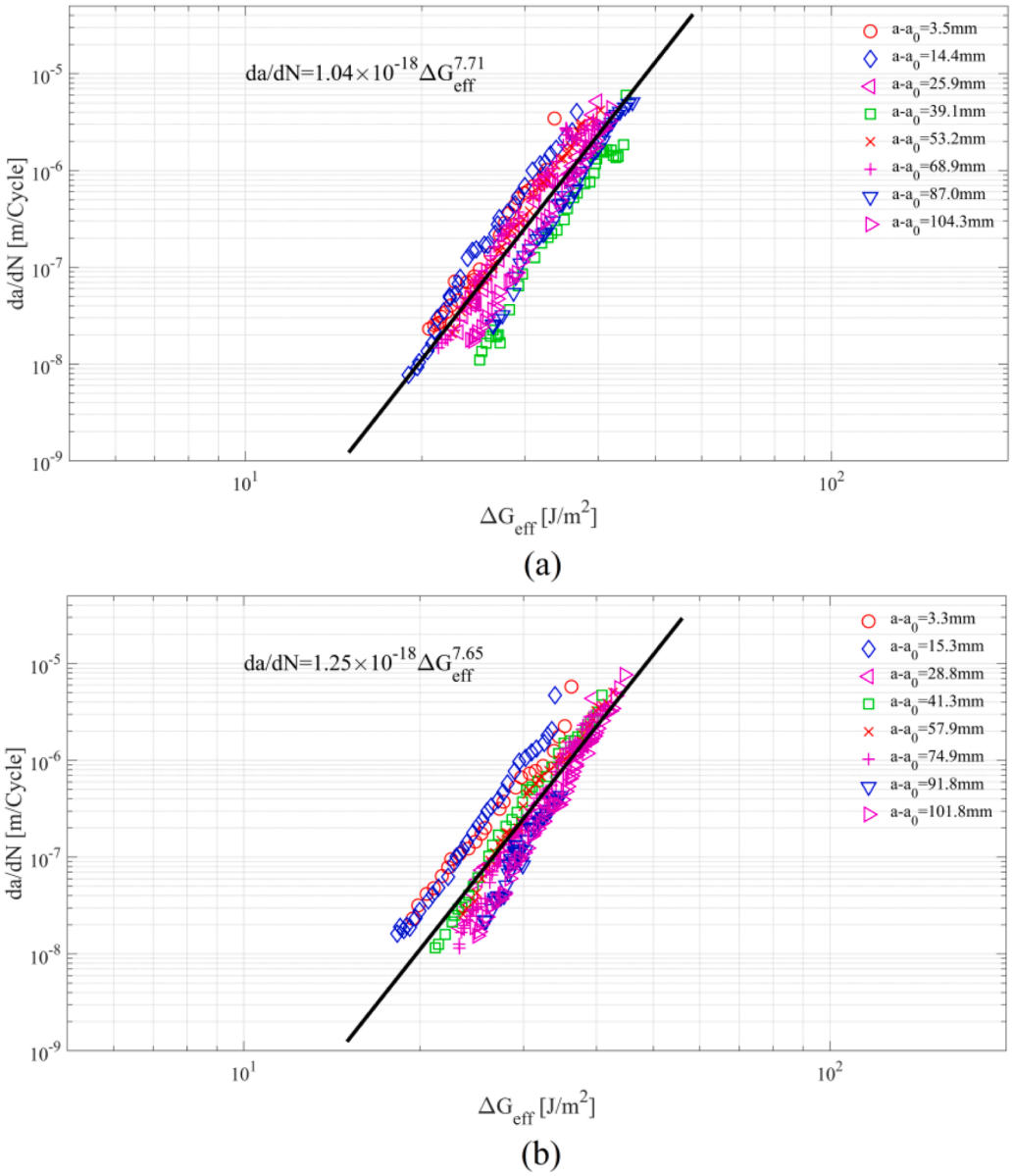

Fig. 9. Fatigue data of 80℃ interpreted via the modified Paris relation. (a) 80℃ Spe-1; (b) 80℃ Spe-2.

delamination resistance at the crack front.

Fig. 10 provides a comparison on the intrinsic mode I FDG behavior at different temperatures. It is clear that elevated temperature can cause the intrinsic FDG acceleration. This temperature dependence indeed agrees well with the initiation delamination resistance results that illustrated in Fig. 6, in which the initiation delamination resistance can decrease with increased temperature.

3.3. Fractographic examinations on FDG at different temperatures

SEM observations were conducted on the fatigue delamination surfaces at different temperatures, to explore the damage mechanisms for temperature dependence of the intrinsic mode I FDG behavior as well as fiber bridging development.

Figs. 11–13 summarize the SEM observation results of fatigue delamination surfaces with different magnification. The fracture morphology was very similar for mode I FDG at RT and elevated 80℃, as shown in Figs. 11 and 12. Particularly, fiber prints, resulting from fiber/matrix interface debonding, is the dominant microscopic feature identified on the fracture surfaces. And no obvious plastic deformation was identified in FDG at RT and 80℃. Accordingly, it is reasonable to draw a conclusion that the damage mechanisms in mode I FDG at RT and 80℃ remain the same. In addition, one should note that elevated temperature not only has detrimental effects on

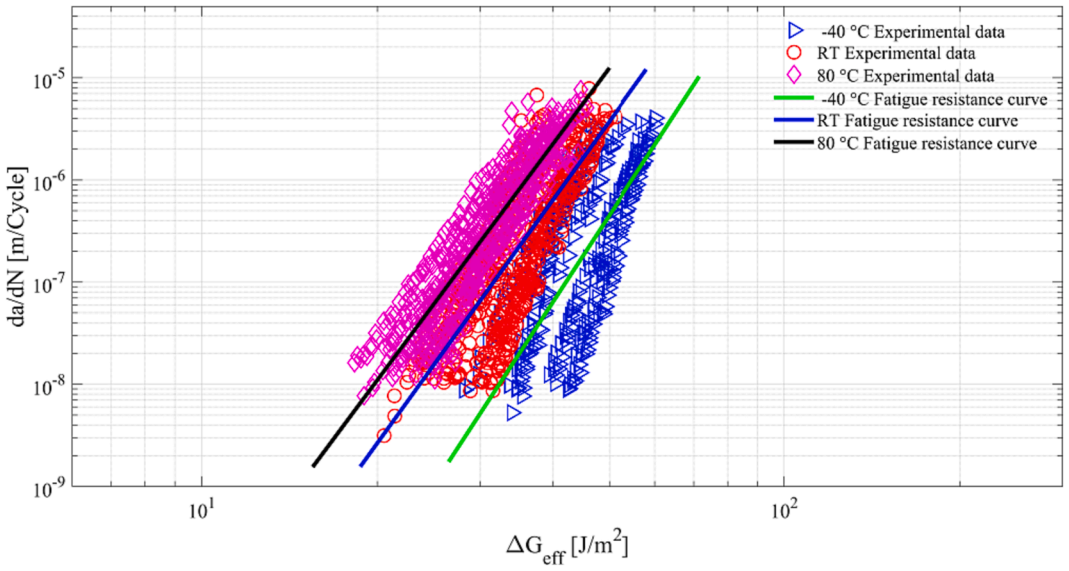

Fig. 10. Temperature effects on the intrinsic mode I FDG behavior in composites.

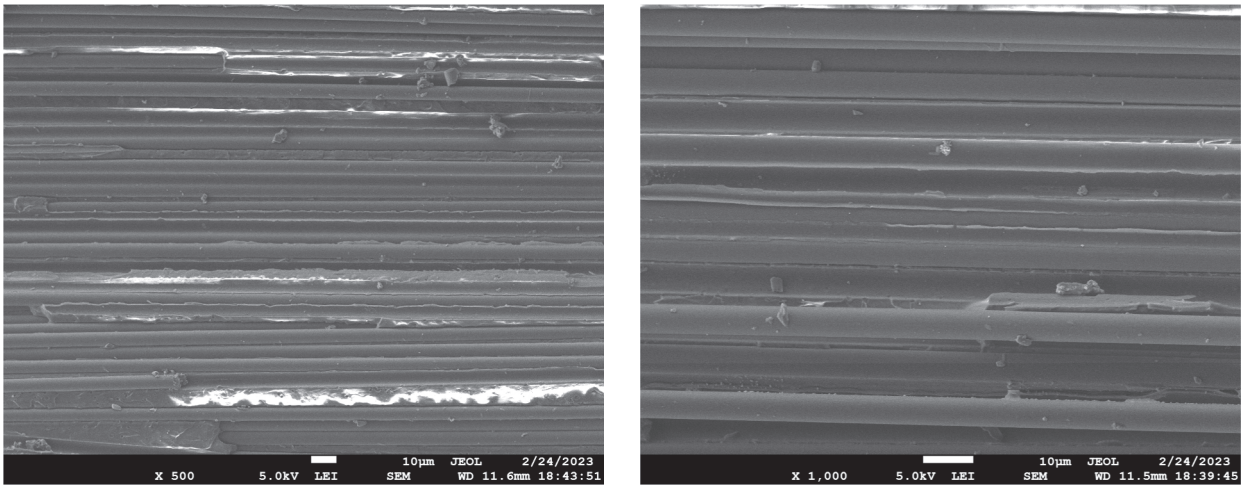

Fig. 11. Fractographic examinations on fracture surface of RT. (a) 500X; (b) 1000X.

fiber/matrix interface adhesion, but also causes matrix yield strength decrease [27]. These changes can promote micro crack/damage formation around fiber/matrix interface region under cyclic loading, and finally cause a faster fatigue crack growth around the delamination front, as illustrated in Fig. 10.

Some important difference was observed on the fatigue delamination surfaces of −40℃, as shown in Fig. 13. In addition to significant fiber prints, matrix brittle fracture failure (marked as hackles, riverlines) was identified at some locations on the delamination surfaces. As discussed in literature [27,35], freezing temperature can promote mechanical interlocking at fiber/matrix interface, i.e. enhancing interface bonding. Furthermore, decreased temperature can also make matrix brittle, and even may cause some micro cracks in the matrix material, thus promoting brittle failure in the matrix [27]. As a result, fatigue propagation at −40℃ is a combination of dominant interface debonding and localized matrix brittle failure. To the authors' opinion, fiber/matrix interface still plays a key role in determining fatigue damage propagation at freezing temperature, finally making mode I intrinsic FDG behavior of −40℃ lower than that of RT and 80℃.

According to the above SEM examinations, FDG behavior at different temperatures is significantly dependent on the performance of fiber/matrix interface. Referring to the fact that the interface adhesion can be enhanced with decreased temperature but weakened with elevated temperature [27,35], hence the mode I intrinsic FDG behavior at the crack front becomes faster with increased

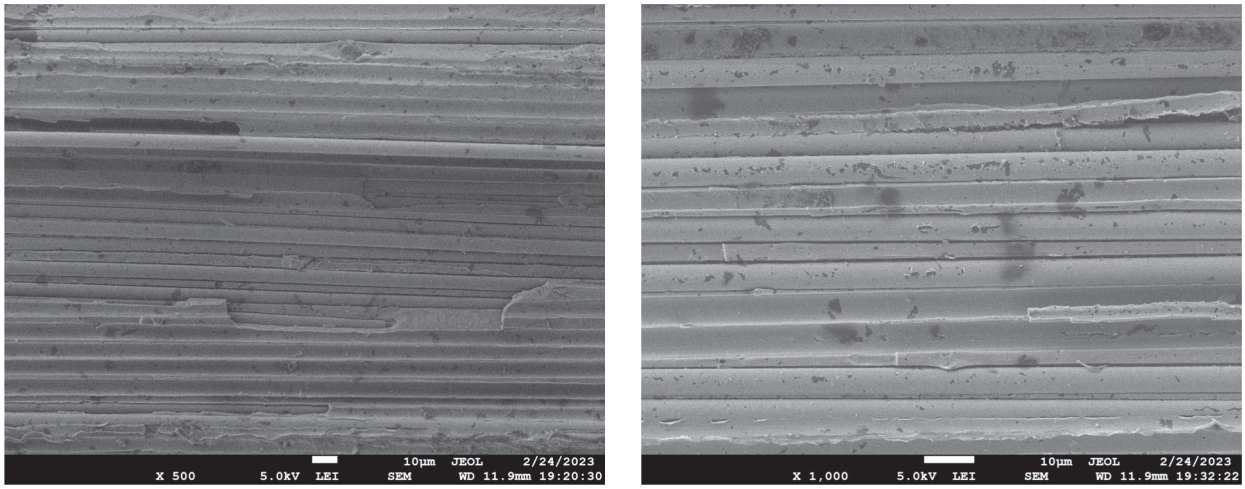

Fig. 12. Fractographic examinations on fracture surface of 80℃. (a) 500X; (b) 1000X.

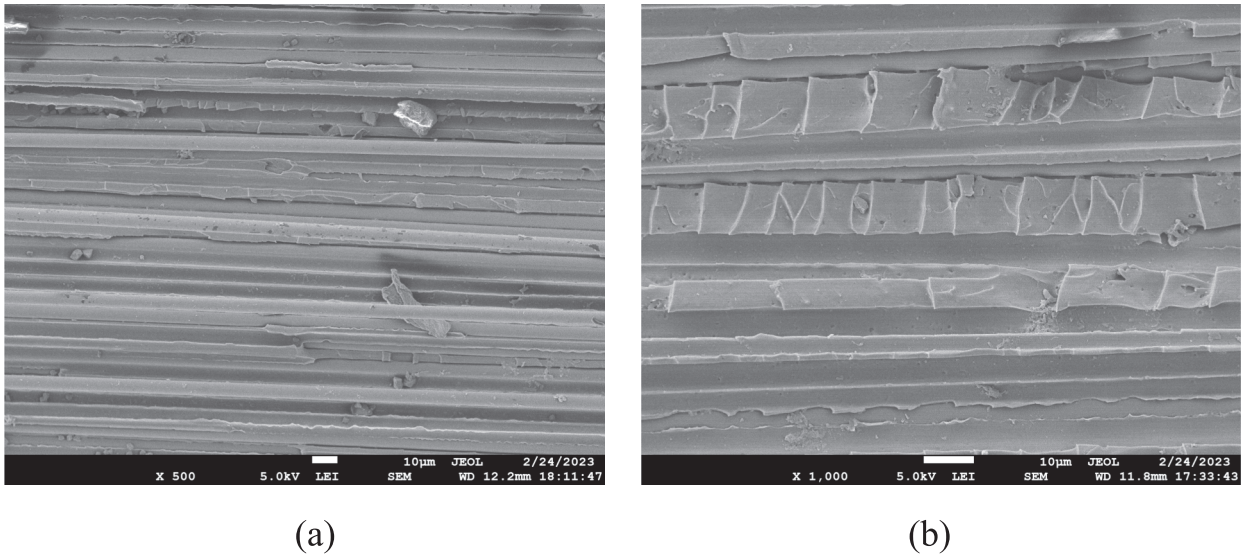

Fig. 13. Fractographic examinations on fracture surface of −40℃. (a) 500X; (b) 1000X.

temperature. Furthermore, it has been reported in literature [7] that weak fiber/matrix interface can promote more bridging fibers during delamination growth. Thus, more bridging fibers can be present in FDG at elevated temperature 80℃, finally contributing to the corresponding *R*-curve with high magnitude as shown in Fig. 6.

3.4. A semi-empirical fatigue delamination model accounting for scatter

According to above discussions, temperature has obvious effects on mode I FDG behavior. Some scatter is observed in FDG data interpretations, as shown in Figs. 7-10. This scatter indeed is unfavorable for composite structural designs. It is therefore reasonable to ask the following question: *how to best determine FDG behavior with consideration of data scatter at different temperatures for engineering designs*.

Referring to using normalization to account for data scatter in a recent study given by Jones et al [19], a new semi-empirical relation Eq.(4) was proposed here to determine mode I FDG behavior at different temperatures.

$$\frac{da}{dN} = C\left(\frac{\Delta G_{eff}}{\Delta G_{da/dN}}\right)^n = C\left[\frac{G_0}{G_{IC}(a-a_0)}\frac{\Delta G}{\Delta G_{da/dN}}\right]^n \tag{4}$$

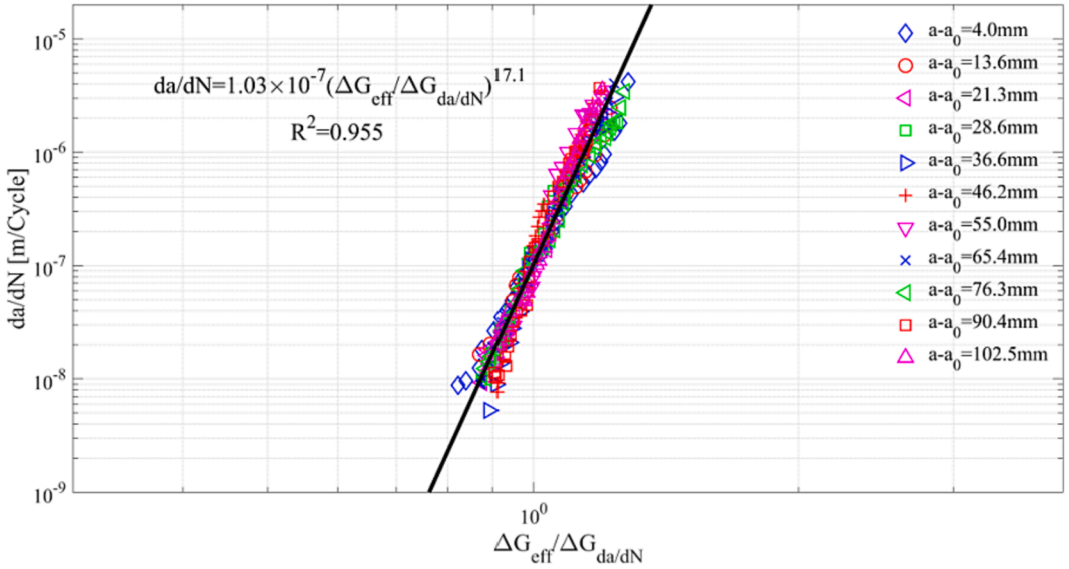

Fig. 14. FDG interpretations of −40℃ via the semi-empirical fatigue model.

where $\Delta G_{da/dN}$ represents the *SERR* of a given *da/dN* using Eq.(2) in fatigue data interpretations. According to the authors' experience, the use of $\Delta G_{da/dN}$ at the magnitude of $da/dN = 1 \times 10^{-7}$m/Cycle can usually lead to good interpretations of the FDG data.

All fatigue data interpreted via Eq.(4) are present in Figs. 14–16. It is clear that the use of this new correlation can significantly reduce data scatter. A single resistance curve with really high determination coefficient (close to unit) can be calibrated to well represent FDG behavior at a given temperature. As discussed by Jones et al [19], the use of normalization indeed force all fatigue data to go through the same point. Referring to the data interpretations illustrated in Figs. 7–9, resistance curves of a given temperature with different crack lengths can have a similar slope. As a result, all fatigue resistance curves can converge into a really narrow band region, and hence reduce data scatter in the entire *SERR* range as shown in Figs. 14–16.

According to the results shown in Figs. 14–16, a regression analysis was conducted on temperature dependence of the model parameters, i.e. *C*, *n* and $\Delta G_{da/dN}$, for the purpose of developing an empirical model to represent FDG behavior at different temperatures. Particularly, it was found that the magnitude of *C* is close equal to 1×10^{-7}. This is reasonable as all resistance curves are forced to pass through the same point at the magnitude of $da/dN = 1 \times 10^{-7}$m/Cycle in the double logarithmic scale, as shown in Figs. 14–16. Good correlations between the averaged *n*, $\Delta G_{da/dN}$ and temperature *T* are obtained, which can nonlinearly decrease with temperature increase as illustrated in Fig. 17. In addition, it was found that the standard deviation of $\Delta G_{da/dN}$ for different temperatures is around 10 % of its mean value. Referring to literature [6], the use of this standard deviation in the fatigue model can account for data scatter.

According to the correlations illustrated in Fig. 17, all parameters required in Eq.(4) for different temperatures can be conveniently determined. And it is assumed here that the standard deviation of $\Delta G_{da/dN}$ at other temperature remains around 10 % of its mean value. Thus, mode I intrinsic FDG behavior at other temperatures with data scatter consideration can be determined. The fatigue data of 50℃ were employed to verify the validity of using Eq.(4) in representing the intrinsic mode I FDG behavior.

Fig. 18 provides the first evidence on the appropriateness of using this methodology in representing the intrinsic FDG behavior. The predicted resistance curves can pass through the central part of the experimental fatigue data. And almost all fatigue data can locate in-between the predicted 99 % confidence intervals. One can therefore make a conclusion that the use of this proposed fatigue model can appropriately determine the mode I intrinsic FDG behavior accounting for data scatter.

4. Concluding remarks

Fiber-bridged mode I FDG behavior in carbon fiber reinforced polymer composite laminates at different temperatures has been thoroughly investigated and discussed in the present study. The following important conclusions can be made:

(1) Temperature has significant effects on fatigue damage propagation at the crack front and fiber bridging development in the wake of the crack front. Particularly, the intrinsic delamination resistance can decrease with increased temperature. Elevated temperature can promote more bridging fibers in FDG, whereas freezing temperature has negligible influence on fiber bridging development.

(2) Fatigue data interpreted via the Paris relation clearly demonstrated that fiber bridging has significant retardation effects on FDG behavior at different temperatures. The calibrated Paris resistance curves can shift downwards and tend to converge into a narrow band region with fiber bridging development.

(3) The use of the modified Paris relation can well determine the damage evolution at the crack front, i.e. the intrinsic Mode I FDG behavior. A master resistance curve can be obtained to represent the intrinsic FDG behavior of a given temperature, agreeing well with

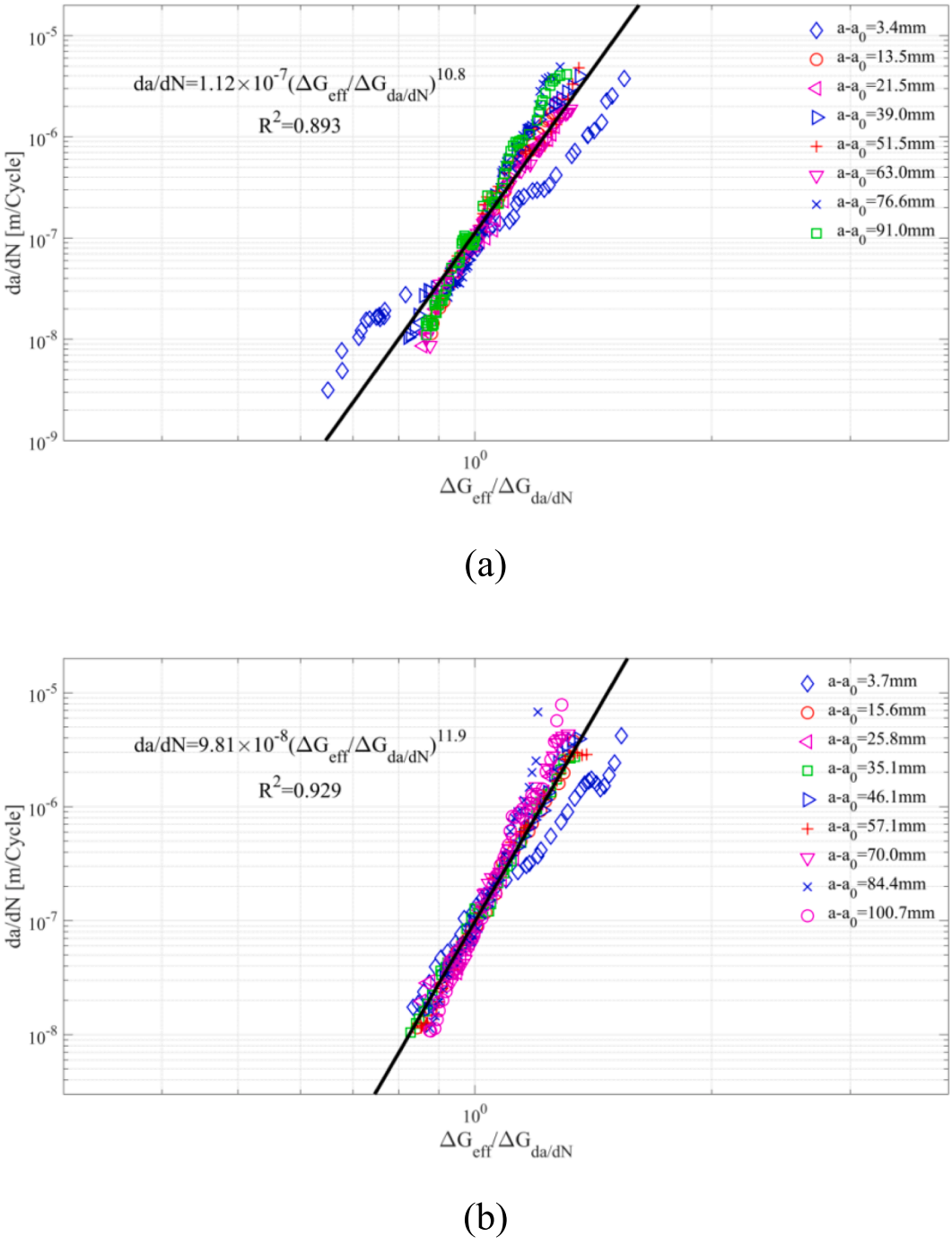

Fig. 15. FDG interpretations of RT via the semi-empirical fatigue model. (a) RT Spe-1; (b) RT Spe-2.

the similitude hypothesis. These data interpretations clearly demonstrated that the intrinsic mode I FDG behavior can accelerate with elevated temperature.

(4) Fractographic observations on delamination fracture surfaces demonstrate that fiber/matrix interface debonding is the dominant damage mechanism in mode I FDG at different temperatures. Increased temperature can weaken interface adhesion, and decreased temperature can enhance interface performance. As a result, the intrinsic mode I delamination resistance decreases with temperature increase. However, weak interface adhesion can promote more bridging fibers during mode I FDG.

(5) A semi-empirical fatigue model, based on normalization, with the capacity of accounting for data scatter has been proposed to represent mode I intrinsic FDG behavior at different temperatures for engineering designs. There is evidence that the application of this

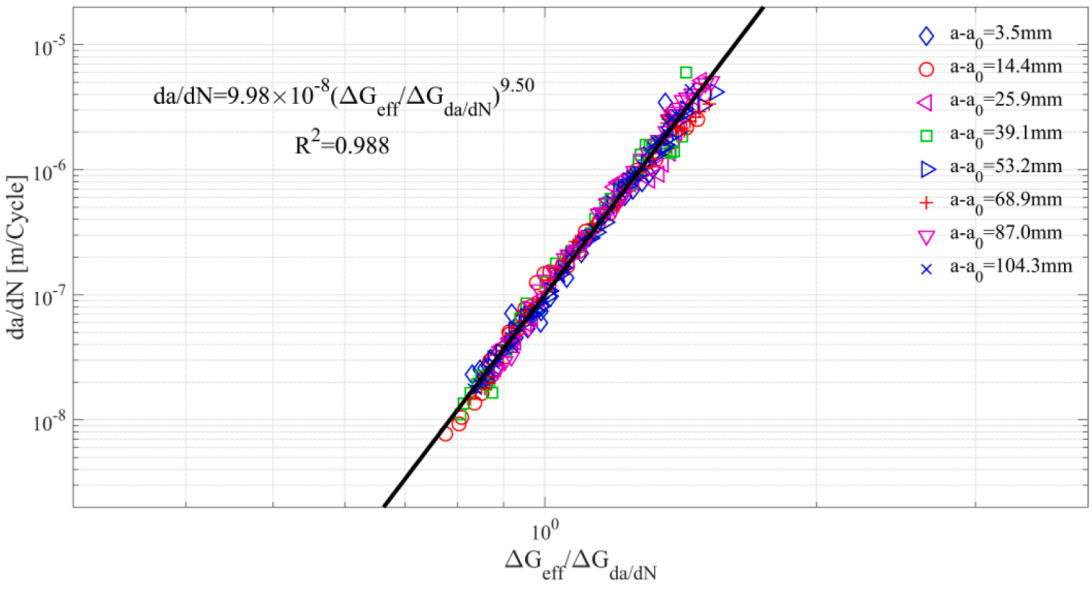

(a)

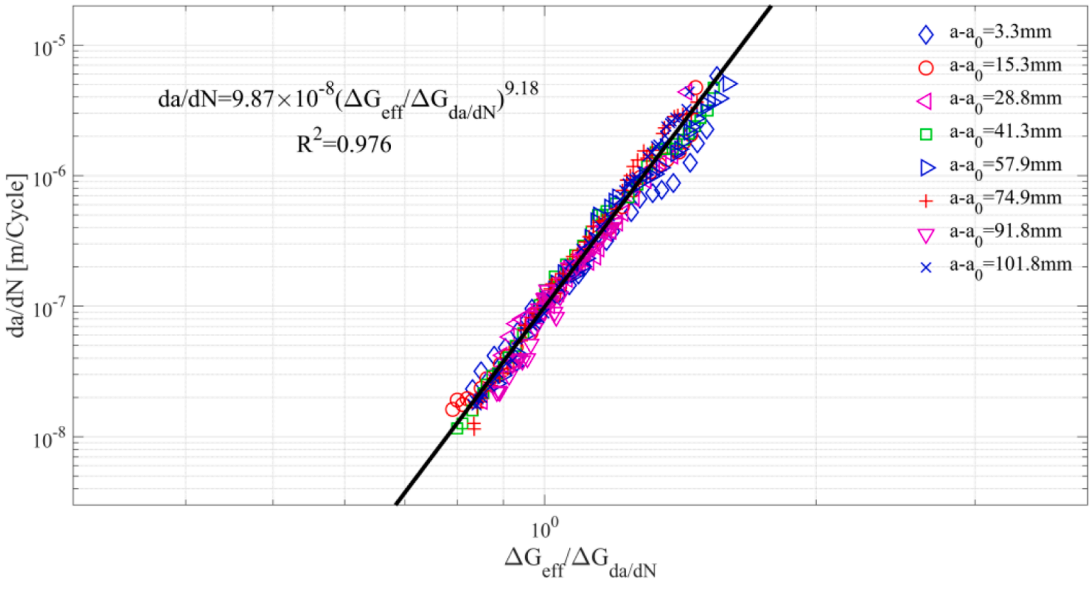

(b)

Fig. 16. FDG interpretations of 80℃ via the semi-empirical fatigue model. (a) 80℃ Spe-1; (b) 80℃ Spe-2.

model can appropriately determine the intrinsic FDG behavior.

(6) This study can provide solid evidence that the modified Paris relation is not only valid at RT, but also effective at freezing and elevated temperatures, in fiber-bridged fatigue delamination data interpretations. This finding will be useful and important for the development of mode I fatigue test standard of composite laminates, aimed by ESIS TC4 and ISO/TC61/SC13.

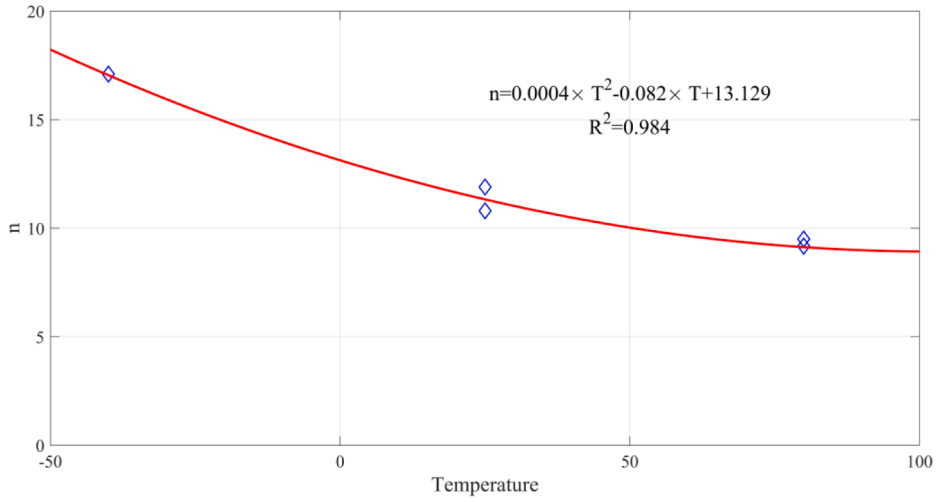

(a)

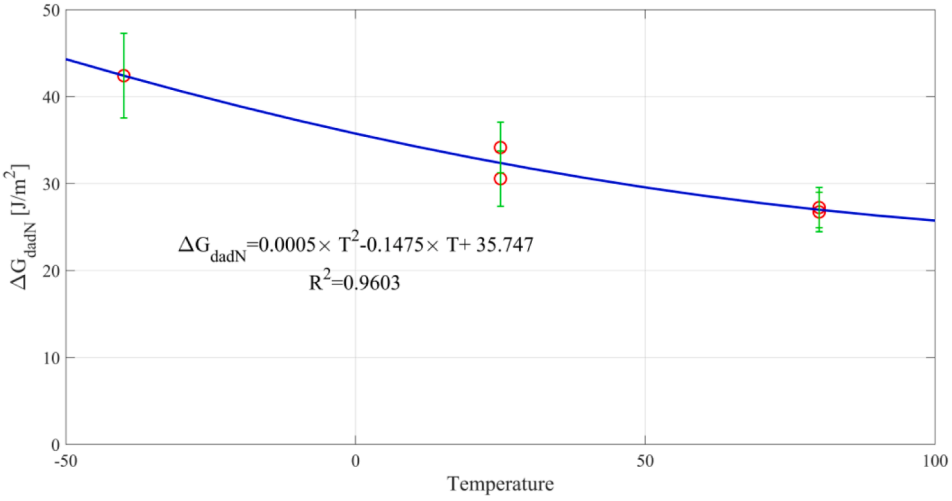

(b)

Fig. 17. Temperature dependence of fatigue model parameters. (a) n vs. T; (b) $\Delta G_{da/dN}$ vs. T.

CRediT authorship contribution statement

Liaojun Yao: Writing – review & editing, Writing – original draft, Visualization, Validation, Supervision, Software, Resources, Project administration, Methodology, Investigation, Funding acquisition, Formal analysis, Data curation, Conceptualization. **Mingyue Chuai:** Visualization, Validation, Software, Methodology, Formal analysis, Data curation. **Hanyue Li:** Software, Formal analysis, Data curation. **Xiangming Chen:** Methodology. **Dong Quan:** Validation, Software, Methodology. **R.C. Alderliesten:** Writing – review & editing. **M. Beyens:** Software, Methodology, Data curation.

Declaration of competing interest

The authors declare that they have no known competing financial interests or personal relationships that could have appeared to influence the work reported in this paper.

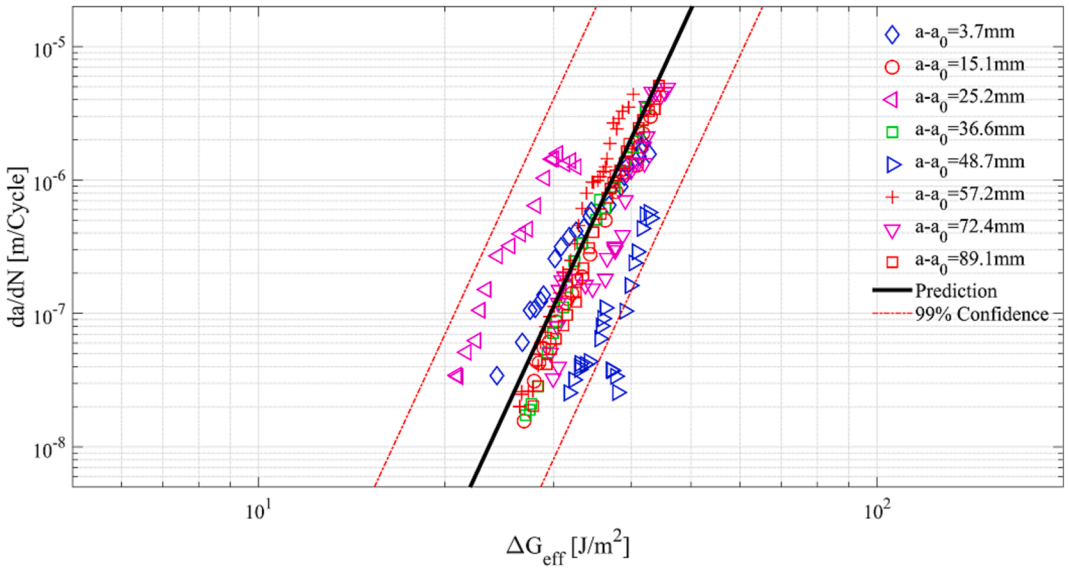

Fig. 18. FDG behavior predictions of 50℃.

Data availability

Data will be made available on request.

Acknowledgement

The authors gratefully acknowledge financial support from the National Natural Science Foundation of China with Grant No. 11902098 and 12272110, the Aeronautical Science Foundation of China with Grant No. 2022Z055077004, the Foundation of the National Key Laboratory of Strength and Structural Integrity with Grant No. ASSIKFJJ202302003, the Natural Science Foundation of Heilongjiang Province with Grant No. LH2020A005, and the Natural Science Foundation of Shandong Province with Grant No. 2022HWYQ-013.

References

[1] Federal Aviation Authority. Airworthiness Advisory Circular No: 20-107B. Composite Aircraft Structure, 2009.
[2] Brunner AJ, Murphy N, Pinter G. Development of a standardized procedure for the characterization of interlaminar delamination propagation in advanced composites under fatigue mode I loading conditions. Engng Fract Mech 2009;76:2678–89.
[3] Stelzer S, Brunner AJ, Arguelles A, Murphy N, Pinter G. Mode I delamination fatigue crack growth in unidirectional fiber reinforced composites: Development of a standardized test procedure. Compos Sci Technol 2012;72:1102–7.
[4] Murri GB. Effect of data reduction and fiber-bridging on mode I delamination characterization of unidirectional composites. J Compos Mater 2014;48:2413–24.
[5] Stelzer S, Brunner AJ, Arguelles A, Murphy N, Cano GM, Pinter G. Mode I delamination fatigue crack growth in unidirectional fiber reinforced composites Results from ESIS TC 4 round-robins. Engng Fract Mech 2014;116:92–107.
[6] Yao L, Alderliesten RC, Jones R, Kinloch AJ. Delamination fatigue growth in polymer-matrix fiber composies: A methodology for determining the design and lifing allowables. Compos Struct 2018;196:8–20.
[7] Khan R. Fiber bridging in composite laminates: A literature review. Compos Struct 2019;229:111418.
[8] Yao L, Alderliesten R, Zhao M, Benedictus R. Bridging effect on mode I fatigue delamination behavior in composite laminates. Compos A Appl Sci Manuf 2014;63:103–9.
[9] Blondean C, Pappas GA, Botsis J. Crack propagation in CFRP laminates under mode I monotonic and fatigue loads: A methodological study. Compos Struct 2021;256:113002.
[10] Shokrieh MM, Hedari-Rarani M, Ayatollahi MR. Delamination R-curve as a material property of unidirectional glass epoxy composites. Mater Des 2012;34:211–8.
[11] Manshadi BD, Farmand-Ashtiani E, Botsis J, et al. An iterative analytical experimental study of bridging in delamination of the double cantilever beam specimen. Compos A Appl Sci Manuf 2014:43–50.
[12] Farmand-Ashtiani E, Cugnoni J, Botsis J. Specimen thickness dependence of large scale fiber bridging in mode I interlaminar fracture of carbon epoxy composite. Int J Solids Struct 2015;55:58–65.
[13] Liu W, Chen P. Delamination in carbon fiber epoxy DCB laminates with different stacking sequences R-curve behavior and bridging. Theor Appl Fract Mech 2020;109:120750.
[14] Bak BLV, Sarrado C, Turon A, Costa J. Delamination under fatigue loads in composite laminates: A review on the observed phenomenology and computational methods. Appl Mech Rev 2014. 060803-1-060803-24.
[15] Hojo M, Ando T, Tanaka M, et al. Modes I and II interlaminar fracture toughness and fatigue delamination of CF epoxy laminate with self-same epoxy interleaf. Int J Fatigue 2006;28:1154–65.
[16] Gong Y, Zhao L, Zhang J, Hu N. A novel model for determining the fatigue resistance in composite laminates from a viewpoint of energy. Compos Sci Technol 2018;167:489–96.
[17] Suo Z, Bao G, Fan B. Determination R-curve phenomena due to damage. J Mech Phys Solids 1992;40:1–16.

[18] Yao L, Alderliesten R, Benedictus R. The effect of fiber bridging on the Paris relation for mode I fatigue delamination growth in composites. Compos Struct 2016; 140:125–35.
[19] Jones R, Peng D, Singh Raman RK, et al. Thoughts on two approaches for accounting for the scatter in fatigue delamination growth curves. Compos Struct 2021; 258:113175.
[20] Peng L, Zhang J, Zhao L, et al. Mode I delamination growth of multidirectional composite laminates under fatigue loading. J Compos Mater 2010;45:1077–90.
[21] Zhang J, Peng L, Zhao L, et al. Fatigue delamination growth rates and thresholds of composite laminates under mixed mode loading. Int J Fatigue 2012;40:7–15.
[22] Jiang L, Zhang Y, Gong Y, et al. A new model characterizing the fatigue delamination growth in DCB laminates with combined effects of fiber bridging and stress ratio. Compos Struct 2021;268:113943.
[23] Yao L, Cui H, Alderliesten RC, Sun Y, Guo L. Thickness effects on fiber-bridged fatigue delamination growth in composites. Compos A Appl Sci Manuf 2018;110: 21–8.
[24] Gregory JR, Spearing SM. A fiber bridging model for fatigue delamination in composite materials. Acta Mater 2004;52:5493–502.
[25] Farmand-Ashtiani E, Cugnoni J, Botsis J. Effects of large scale bridging in load controlled fatigue delamination of unidirectional carbon-epoxy specimens. Compos Sci Technol 2016;137:52–9.
[26] Yao L, Sun Y, Guo L, Zhao M, Jia L, Alderliesten RC, et al. A modified Paris relation for fatigue delamination with fiber bridging in composite laminates. Compos Struct 2017;176:556–64.
[27] Charalambous G, Allegri G, Hallett SR. Temperature effects on mixed mode I/II delamination under quasi-static and fatigue loading of a carbon/epoxy composite. Compos A Appl Sci Manuf 2015;77:75–86.
[28] Coronado P, Arguelles A, Vina J, Vina I. Influence of low temperatures on the phenomenon of delamination of mode I fracture in carbon-fiber/epoxy composites under fatigue loading. Compos Struct 2014;112:188–93.
[29] Gregory JR, Spearing SM. Constituent and composite quasi-static and fatigue fracture experiments. Compos A Appl Sci Manuf 2005;36:665–74.
[30] Sjogren A, Asp LE. Effects of temperature on delamination growth in a carbon/epoxy composite under fatigue loading. Int J Fatigue 2002;24:179–84.
[31] R. Rodi. The residual strength failure sequence in fiber metal laminates. PhD thesis of Delft University of Technology, 2012.
[32] Jones R, Molent L, Pitt S. Similitude and the Paris crack growth law. Int J Fatigue 2008;30:1873–80.
[33] Jones R, Kinloch AJ, Michopoulos J, Iliopoulos AP. Crack growth in adhesives: Similitude and the Hartman-Schijve equation. Compos Struct 2021;273:114260.
[34] Cano AJ, Salazar A, Rodriguez J. Evaluation of different crack driving forces for describing the fatigue crack growth behavior of PET-G. Int J Fatigue 2018;107: 27–32.
[35] Hartwig G, Knaak S. Fiber-epoxy composites at low temperature. Cryogenics 1984;24:639–47.